

Nonlocal Second Order Vehicular Traffic Flow Models And Lagrange-Remap Finite Volumes

Florian De Vuyst, Valeria Ricci, and Francesco Salvarani

Abstract In this paper a second order vehicular macroscopic model is derived from a microscopic car-following type model and it is analyzed. The source term includes nonlocal anticipation terms. A Finite Volume Lagrange–remap scheme is proposed.

Keywords Vehicular traffic flow, modeling, car-following, microscopic, macroscopic, finite volumes, Lagrange–remap

MSC2010: 65M08, 65M22, 65P40, 65Y20, 65Z05

1 Motivation and introduction

There are many ways to describe and model a vehicular traffic flow. Microscopic models e.g. [3] describe the interaction between two successive vehicles. It is known that car-following models may have a complex dynamics (see for example [8, 9]) and are able to reproduce all the flow regimes. In the macroscopic models, conservation laws and balance equations on mean quantities are searched. Since the pioneer works by Lighthill, Whitham and Richards (LWR model), numerous improvements and contributions have been proposed. In 2000, Aw and Rascle [1] derived an interesting second order model that fixed the drawbacks of Payne's

Florian De Vuyst

Centre de Mathématiques et de leurs Applications, École Normale Supérieure de Cachan, 61 avenue du Président Wilson, 94235 Cachan France, e-mail: devuyst@cmla.ens-cachan.fr

Valeria Ricci

Dipartimento di Metodi e Modelli Matematici Universita' di Palermo, Viale delle Scienze, Edificio 8, 90128 Palermo, Italy, e-mail: valeria.ricci@unipa.it

Francesco Salvarani

Dipartimento di Matematica, Università degli Studi di Pavia, Via Ferrata 1 - I-27100 Pavia, Italy, e-mail: francesco.salvarani@unipv.it

model, emphasized by Daganzo [4]. More recently, Aw et al. [2] derived the Aw–Rascle model from microscopic follow-the-leader models. Illner et al. [7] were also able to retrieve the Aw–Rascle model from a kinetic Vlasov description. For related works, see for example [5,6]. In this paper, a continuum traffic flow model is derived from a more complex car-following model.

2 Car-following rule and microscopic model

Let us consider a vehicular traffic flow made of N vehicles, indexed by i , $i = 1, \dots, N$. For simplicity, we will assume that all the vehicles are identical, of length ℓ . The car indexed by i follows the car $(i + 1)$. At time t , the vehicle i is located at position $x_i(t)$ with speed $\dot{x}_i = v_i$. The spatial gap between the two vehicles i and $(i + 1)$ is then given by $x_{i+1}(t) - x_i(t) - \ell$ (see Fig. 1). The maximum (permitted) speed will be denoted by v_M . Let us also denote by $g^s(v_i, v_{i+1})$ the safety spatial gap for the vehicle i , depending on the vehicle speeds i and $(i + 1)$. A simple relaxation rule for the spatial gap is

$$\frac{d}{dt}(x_{i+1} - x_i - \ell) = \frac{g^s(v_i, v_{i+1}) - (x_{i+1} - x_i - \ell)}{x_{i+1} - x_i - \ell} a_{i,i+1} \quad (1)$$

where $a_{i,i+1}$ is a local characteristic speed. The denominator forbids the collision between the two vehicles. Then we get a target speed v_i^{target} equal to

$$v_i^{target} = v_{i+1} + \left(1 - \frac{g^s(v_i, v_{i+1})}{x_{i+1} - x_i - \ell}\right) a_{i,i+1}. \quad (2)$$

A simple acceleration rule toward the target speed is given by the relaxation scheme

$$\frac{dv_i}{dt} = \frac{v_i^{target} - v_i}{\lambda} = \frac{v_{i+1} - v_i}{\lambda} + \left(1 - \frac{g^s(v_i, v_{i+1})}{x_{i+1} - x_i - \ell}\right) \frac{a_{i,i+1}}{\lambda} \quad (3)$$

using a characteristic relaxation time $\lambda > 0$. Let us comment three interesting cases. If $0 < x_{i+1} - x_i - \ell \ll 1$, then there is a strong breaking in order not to collide. If $x_{i+1} - x_i - \ell \equiv g^s(v_i, v_{i+1})$, the vehicle i is at the right safe distance, and in that case we have the simple car-following rule $\dot{v}_i = (v_{i+1} - v_i)/\lambda$. If $x_{i+1} - x_i \gg 1$,

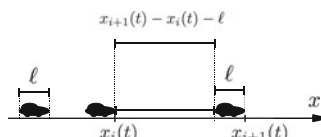


Fig. 1 Microscopic description of the vehicular traffic

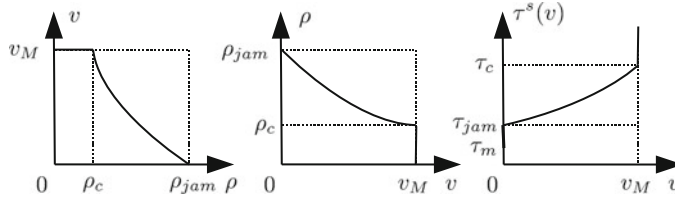


Fig. 2 Fundamental diagram of traffic flow and link with the spatial safety gap

the vehicle's driver i should not be worried about vehicle $(i + 1)$ because it is too far from him. In that case, the driver i should accelerate up to the limit speed v_M according to the rule $\dot{v}_i = (v_M - v_i)/\lambda$. This suggests us to choose $a_{i,i+1} = v_M - v_{i+1}$. To summarize, we get the microscopic model

$$\frac{dv_i}{dt} = \frac{v_{i+1} - v_i}{\lambda} + \left(1 - \frac{g^s(v_i, v_{i+1})}{x_{i+1} - x_i - \ell}\right) \frac{v_M - v_{i+1}}{\lambda}. \quad (4)$$

3 Macroscopic quantities and spatial safety gap

From the microscopic quantities, one can define some macroscopic ones. The specific volume $\tau_{i+1/2}(t) := x_{i+1}(t) - x_i(t)$ has the dimension of a length. The density $\rho_{i+1/2}(t) = (\tau_{i+1/2}(t))^{-1}$ returns the local number of vehicles per unit length. The quantity $\rho_M = \ell^{-1}$ represents the maximum density (nose-to-tail vehicles) and $\tau_m = \ell$ is the minimum specific volume. Now in (4), we need a closure for the safety gap function g^s . From g^s one can define a safety specific volume τ^s such that $g^s = \tau^s - \ell = \tau^s - \tau_m$ and a safety density $\rho^s = (\tau^s)^{-1}$. The density ρ^s can be identified to the fundamental diagram of traffic flow which gives a relation between the density and the equilibrium (safe) speed (see Fig. 2). We shall here consider

$$g^s(v_i, v_{i+1}) = \tau^s\left(\frac{v_i + v_{i+1}}{2}\right) - \tau_m.$$

4 Macroscopic model

In order to derive a macroscopic model, let us introduce some interpolation functions $v(x, t)$ and $\tau(x, t)$ such that

$$v(x_i(t), t) = v_i(t), \quad \tau(x_{i+1/2}(t), t) = x_{i+1}(t) - x_i(t) \quad \forall i = 1, \dots, N.$$

A Taylor expansion allows us to write

$$v_{i+1}(t) - v_i(t) = v(x_{i+1}(t), t) - v(x_i(t), t) = \left(\tau \frac{\partial v}{\partial x} \right) (x_{i+1/2}(t), t) + o((x_{i+1} - x_i)^2).$$

From the motion equation $\dot{x}_i = v_i$, one can write $\frac{d}{dt}(x_{i+1}(t) - x_i(t)) = v_{i+1}(t) - v_i(t)$. Then we have

$$\frac{D\tau}{Dt}(x_{i+1/2}(t), t) = \frac{\partial v}{\partial x}(x_{i+1/2}(t), t) \tau(x_{i+1/2}(t), t) + o((x_{i+1}(t) - x_i(t))^2).$$

We omit the remaining term and consider that the expression holds almost everywhere, then we get the continuity equation

$$\rho \frac{D\tau}{Dt} - \frac{\partial v}{\partial x} = 0 \quad \Leftrightarrow \quad \frac{\partial \rho}{\partial t} + \frac{\partial}{\partial x}(\rho v) = 0. \quad (5)$$

Consider now the acceleration equation. First remark that

$$\left(\frac{\partial v}{\partial x} \tau \right) (x_{i+1/2}(t), t) = \left(\frac{\partial v}{\partial x} \tau \right) (x_i(t), t) + \frac{\tau}{2} \frac{\partial}{\partial x} \left(\tau \frac{\partial v}{\partial x} \right) (x_i(t), t) + o(x_{i+1} - x_i).$$

One can also write $v_{i+1}(t) = v(x_{i+1}(t), t) = v(x_i(t) + \tau(x_{i+1/2}(t), t), t)$, which allows us to derive the balance equation in Lagrangian form

$$\rho \frac{Dv}{Dt} = \frac{1}{\lambda} \frac{\partial v}{\partial x} + \frac{1}{2\lambda} \frac{\partial}{\partial x} \left(\tau \frac{\partial v}{\partial x} \right) + \left(1 - \frac{g^s(v(x + \tau/2, t))}{\tau - \tau_m} \right) \rho \frac{v_M - v(x + \tau, t)}{\lambda}. \quad (6)$$

i.e. in Eulerian form

$$\frac{\partial}{\partial t}(\rho v) + \frac{\partial}{\partial x} \left(\rho v^2 - \frac{1}{\lambda} v \right) - \frac{1}{2\lambda} \frac{\partial}{\partial x} \left(\tau \frac{\partial v}{\partial x} \right) = \left(1 - \frac{g^s(v(x + \tau/2, t))}{\tau - \tau_m} \right) \rho \frac{v_M - v(x + \tau, t)}{\lambda}. \quad (7)$$

By multiplying formally equation (6) by v and using the continuity equation we get

$$\begin{aligned} & \frac{\partial}{\partial t}(\rho v^2/2) + \frac{\partial}{\partial x} \left(\rho v^3/2 - \frac{1}{\lambda} v^2/2 \right) - \frac{1}{2\lambda} \frac{\partial}{\partial x} \left(\tau \frac{\partial(v^2/2)}{\partial x} \right) \\ & - \left(1 - \frac{g^s(v(x + \tau/2, t))}{\tau - \tau_m} \right) \rho v \frac{v_M - v(x + \tau, t)}{\lambda} = -\frac{1}{2\lambda} \tau \left(\frac{\partial v}{\partial x} \right)^2. \end{aligned} \quad (8)$$

This shows that $S = \rho v^2/2$ is an entropy for the system. It is easy to show that S is convex with respect to the conservative variables $(\rho, \rho v)$ (but not strictly convex). More generally, for any \mathcal{C}^2 strictly convex function $h : \mathbb{R}^+ \rightarrow \mathbb{R}^+$, the function $S = \rho h(v)$ is a (non strictly) convex entropy for the system.

Properties Let us consider the first order homogeneous part of the system, i.e.

$$\partial_t \rho + \partial_x(\rho v) = 0, \quad \partial_t(\rho v) + \partial_x(\rho v^2 - \frac{1}{\lambda} v) = 0. \quad (9)$$

In primitive variables (τ, v) we get

$$\partial_t(\tau, v)^T + \begin{pmatrix} v & -\tau \\ 0 & (v - \frac{\tau}{\lambda}) \end{pmatrix} \partial_x(\tau, v)^T = 0.$$

The system is strictly hyperbolic in the admissible space $\Omega_\varepsilon^{ad} = \{(\rho, v), \rho \in [\varepsilon, \rho_M], v \in [0, v_M]\}$ for any $\varepsilon > 0$. The characteristic speeds are $\lambda_1 = v$ and $\lambda_2 = v - \tau/\lambda$. It is easy to check that the two characteristic fields are both linearly degenerate (LD) so that the eigenvalues of the system $\lambda_i, i = 1, 2$ are the Riemann invariants. One gets a straightforward structure of the solutions of the Riemann problem made of two contact discontinuities.

5 Finite volume scheme

For the sake of simplicity, we shall only deal with the inviscid part of the system above. Let us consider a uniform discretization of the spatial domain (with constant mesh step h) made of discrete points $(x_j)_{j \in \mathbb{Z}}$, $x_{j+1} = x_j + h$ and cells $I_j = (x_{j-1/2}, x_{j+1/2})$, $x_{j+1/2} = (x_j + x_{j+1})/2$. From time t^n , the time advance is performed using a time step Δt^n subject to stability constraints that will be detailed later on. The numerical discretization here follows ideas from Billot et al. [5].

Homogeneous Part Because of the structure of the eigenwaves in (9), a Lagrange–remap conservative FV approach is particularly well suited. Initially the discrete solution is piecewise constant on each control volume I_j with density ρ_j^n , specific volume $\tau_j^n = (\rho_j^n)^{-1}$, and speed v_j^n . In the Lagrange step, the computational grid moves according to the flow; the states into each cell evolve according to the Lagrangian equations. For an initial volume $I_j = (x_{j-1/2}, x_{j+1/2})$, the interface points $x_{j-1/2}$ are moved according to the motion equations $\dot{x}_{j+1/2} = v_{j+1/2}^n$ over a time step Δt^n : this gives $x_j^{n+1,-} = x_j^n + \Delta t^n v_{j+1/2}^n$. The choice $v_{j+1/2}^n = v_{j+1}^n$ is compatible with the structure of the solutions of the local Riemann problems, leading to a stable upwind process. After a time step, the cell sizes $h_j^{n+1,-}$ become

$$h_j^{n+1,-} = h + \Delta t^n (v_{j+1}^n - v_j^n). \quad (10)$$

The continuity equation shows that the number of vehicles m_j into each Lagrangian cell I_j is conserved, i.e. $m_j^n = \rho_j^n h = \rho_j^{n+1,-} h_j^{n+1,-} = m_j^{n+1,-}$. Combining (10) and mass conservation, we get the equivalent script

$$\tau_j^{n+1,-} = \tau_j^n + \frac{\Delta t^n}{h} \left(v_{j+1}^n - v_j^n \right). \quad (11)$$

The CFL-like condition forbids the 1-waves to interact with the moving interfaces:

$$\frac{\Delta t^n}{h} \sup_{j \in \mathbb{Z}} \left[v_j^n - \min(0, v_j^n - \frac{\tau_j^n}{\lambda}) \right] \leq 1. \quad (12)$$

By defining

$$v_j^{n+1,-} = \frac{\int_{I_j^{n+1,-}} \rho^{n+1,-}(x) v^{n+1,-}(x) dx}{\int_{I_j^{n+1,-}} \rho^{n+1,-}(x) dx} = \frac{\int_{I_j^{n+1,-}} \rho^{n+1,-}(x) v^{n+1,-}(x) dx}{m_j^n}$$

the speed in the cell $I_j^{n+1,-}$ before projection, we get the following scheme

$$v_j^{n+1,-} = v_j^n + \frac{\Delta t^n}{m_j^n \lambda} \left(v_{j+1}^n - v_j^n \right). \quad (13)$$

The Lagrange phase is followed by a conservative projection onto the initial uniform mesh. Denoting by $\alpha_{j+1/2}^n = v_{j+1}^n \Delta t^n / h$ the local Courant number related to the flow speed, the projection of the density in the cell I_j reads

$$\rho_j^{n+1} = \alpha_{j-1/2}^n \rho_{j-1}^{n+1,-} + \left(1 - \alpha_{j-1/2}^{n+1,-} \right) \rho_j^{n+1,-} \quad (14)$$

as soon as the time step Δt^n satisfies the additional CFL condition $\frac{\Delta t^n}{h} \sup_{j \in \mathbb{Z}} v_j^n \leq 1$. Similarly, the projection of the conservative quantity (ρv) writes

$$(\rho v)_j^{n+1} = \alpha_{j-1/2}^n (\rho v)_{j-1}^{n+1,-} + \left(1 - \alpha_{j-1/2}^{n+1,-} \right) (\rho v)_j^{n+1,-} \quad (15)$$

and gives v_j^{n+1} . It is easy to prove that this numerical scheme fulfills a discrete entropy inequality for the family of entropy functions $S = \rho h(v)$.

Source Term Integration The second equation has a source term that acts as a speed relaxation toward the maximum speed v_m in the case a free flow regime. The differential problem to solve is

$$\frac{dv}{dt} = \left(1 - \frac{g^s(v(x + \tau/2, t))}{\tau - \tau_m} \right) \frac{v_M - v(x + \tau, t)}{\lambda}. \quad (16)$$

When spatially discretized, we have to solve the differential problem

$$\frac{dv_j}{dt} = \left(1 - \frac{g^s(v(x_j + \tau_j/2, t))}{\tau_j - \tau_m} \right) \frac{v_M - v(x_j + \tau_j, t)}{\lambda}, \quad v_j(0) = v_j^0. \quad (17)$$

The problem (17) is nonstandard because of the presence of delays, nonlocal terms (due to the anticipation by the drivers) but also the coupling between the space variable x and the specific volume τ . A computational approach for (17) requires an interpolation of the function v , such as piecewise linear interpolation for example. If, from the discrete point of view, one expects a local influence of the anticipation, we have to assume that h is “large enough” to fulfill the inequality

$$\inf_{j \in \mathbb{Z}} \rho_j^n \geq h^{-1}. \quad (18)$$

The condition (18) may appear surprising, but actually it expresses that the spatial discretization must be compatible with the maximum space headway. As example, consider a road section of length $L = 200$ km and a uniform mesh made of $M = 1000$ points. Then $h = L/M = 0.2$ km and $h^{-1} = 5$ km $^{-1}$. The discretization of the source term may be local as soon as the vehicle density does not go below 5 veh/km.

Whole Fractional Step Method A consistent second–order accurate time splitting of the full inhomogeneous system may be achieved using the Strang fractional step approach. Each time iteration is made of three substeps: (i) a time integration of the source term over a time step $\Delta t^n/2$; (ii) a time advance of the homogeneous system over a time step Δt^n , (iii) a time integration of the source term over Δt^n as in (i).

6 Numerical experiments

In this experiment we use $v_M = 130$, a section length $L = 200$, a uniform mesh composed of 500 points, $\lambda = 4/3600$ and $\rho_M = 260$. We use periodic boundary conditions. The safety density is chosen as

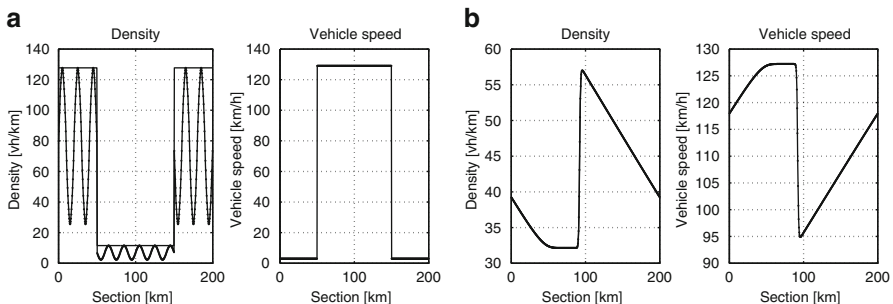


Fig. 3 (a) Initial condition: density (left) and speed (right). (b) Discrete solution at final time: density (left) and speed (right)

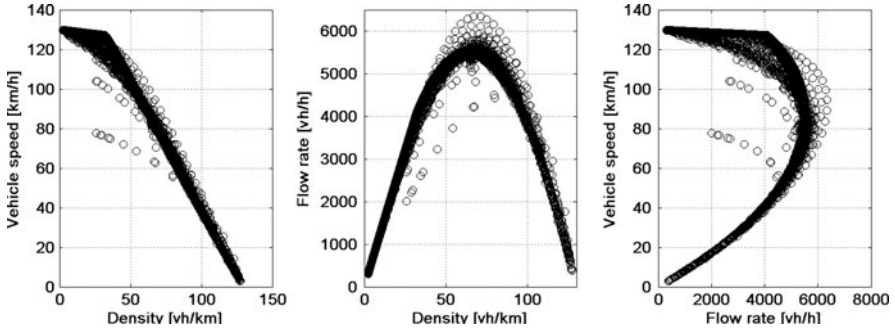


Fig. 4 Discrete solution in the phase space. From left to right: (ρ, v) , $(\rho, \rho v)$ and $(\rho v, v)$ diagram

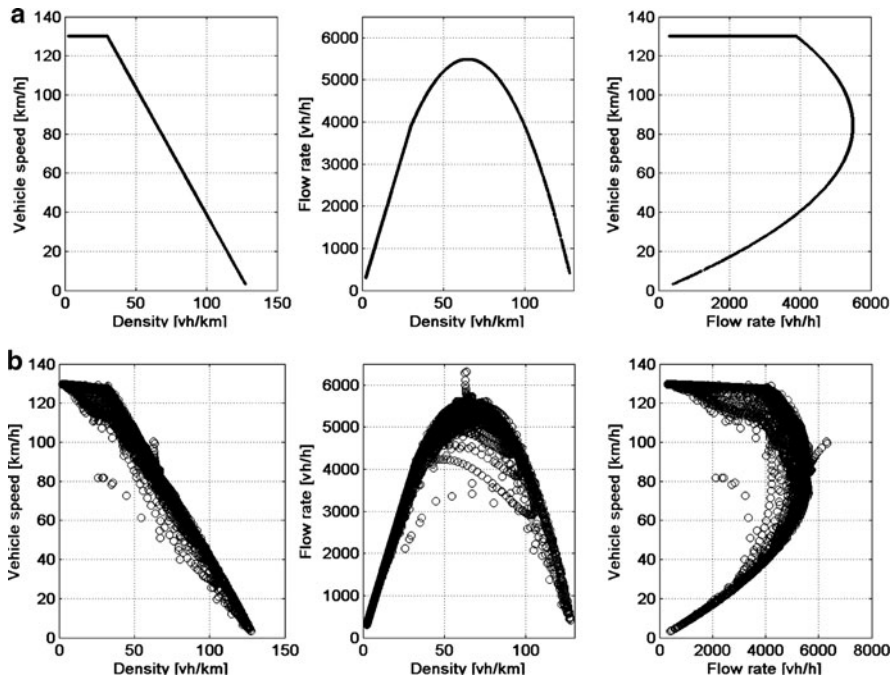


Fig. 5 Numerical Fundamental Diagram computed with: (a) LWR model, (b) Aw–Rascle model

$$\rho^s(v) = \min \left(1500 \frac{v_M - v}{v_M}, \rho_{jam} + (\rho_c - \rho_{jam}) \frac{v}{v_M} \right)$$

with $\rho_c = 30$ and $\rho_{jam} = 130$. The initial velocity field is a piecewise constant function equal to 3 on $[0, L/4] \cup [3L/4, L]$ and equal to 129 on the interval $(L/4, 3L/4)$. The initial density profile $\rho^0(x) = (0.6 + 0.4 \sin(20\pi x/L)) \rho^s(v)$ mimics some nonequilibrium and traffic instabilities (see Fig. 3 (a)). On Fig. 3 (b),

the discrete solution at final simulation time $t = 2.22$ is plotted and shows a very good behaviour of the numerical scheme with strong numerical stability, particularly through shock waves. Figure 4 shows the discrete solution for all discrete times in the phase space. One can observe a very good agreement with what is physically expected. The computed numerical discrete fundamental diagram is compared to those obtained with the LWR and Aw–Rascle models, respectively. For the Aw–Rascle model $\partial_t \rho + \partial_x(\rho v) = 0$, $\partial_t v + (v - \rho p'(\rho))\partial_x v = \frac{A}{T}(v^{eq}(\rho) - v)$, we used $v^{eq}(\rho) = \min\left(v_M(1 - \frac{\rho}{1500}), v_M - v_M \frac{\rho - \rho_c}{\rho_{jam} - \rho_c}\right)$, $p(\rho) = v_M - v^{eq}(\rho)$, $A = 1$, $T = \lambda$.

References

1. A. Aw and M. Rascle, *Resurrection of “second order” models of traffic flow*. SIAM J. Appl. Math., Vol. 60 (3), (2000), 916–938.
2. A. Aw, A. Klar, T. Materne, and M. Rascle. Derivation of continuum traffic flow models from microscopic follow-the-leader models, SIAM J. Applied Math., 63 (1), 259–278 (2002).
3. M. Bando, K. Hasebe, A. Nakayama, A. Shibata, Y. Sugiyama, Phys. Rev. E 51, 1035 (1995).
4. C. F. Daganzo, *Requiem for second order fluid approximations of traffic flow*, Transp. Research B, 29, (1995), 277–286.
5. R. Billot, C. Chalons, F. De Vuyst, N. E. El Faouzi, J. Sau, A conditionally linearly stable second-order traffic model derived from a Vlasov kinetic description, Comptes Rendus Mécanique, Volume 338 (9) (2010), 529–537.
6. D. Helbing and A. Johansson, *On the controversy around Daganzos requiem for and Aw–Rascle’s resurrection of 2nd-order traffic flow models*, Eur. Phys. J. B 69(4), (2009), 549–562.
7. R. Illner, C. Kirchner and R. Pinna, *A Derivation of the Aw–Rascle traffic models from the Fokker–Planck type kinetic models*, Quart. Appl. Math. 67, (2009), 39–45.
8. B.S. Kerner, Springer, Berlin, New York (2009).
9. E. Tomer, L. Safonov and S. Havlin, Presence of Many Stable Nonhomogeneous States in an Inertial Car-Following Model, Phys. Rev. Lett. 84 (2), 382385 (2000).

The paper is in final form and no similar paper has been or is being submitted elsewhere.